First-order induced Raman scattering from Ni^{2+} ions and cation vacancies in LiCl†

J. B. Bates, R. F. Wood, G. E. Shankle,* and Mark Mostoller
Solid State Division, Oak Ridge National Laboratory, Oak Ridge, Tennessee 37830
(Received 12 November 1976)

First-order induced Raman scattering has been observed from single crystals of LiCl containing Ni^{2+} ions. Sharp bands at 247, 216, 161, and 122 cm^{-1} are assigned to A_{1g}, T_{2g}, E_g, and T_{2g} modes, respectively, on the basis of polarization measurements with ⟨100⟩ and ⟨110⟩ crystals. No differences were observed in the experimental peak positions, bandwidths, or relative intensities for crystals in which the Ni^{2+} concentration differed by a factor of 2. Theoretical calculations suggest that the A_{1g} and the higher frequency T_{2g} bands are due to vibrations about the Ni^{2+} ions, while the E_g and possibly the lower-frequency T_{2g} bands can be assigned to the local modes about the cation vacancies.

I. INTRODUCTION

First-order Raman scattering is normally forbidden by symmetry in alkali-halide crystals. However, introduction of a substitutional-impurity ion into the cubic lattice destroys the translational symmetry, and Raman scattering from vibrational motion of the neighbors of the impurity ion can be observed. In simple terms, the scattering can be viewed as arising from the *gerade* normal modes of an MX_6 octahedral species, where M is the substitutional impurity surrounded by six nearest-neighbor ions X. The observed frequencies and band shapes depend on the M-X force constants and on the interaction of the MX_6 unit with the surrounding lattice. Many experimental[1] and theoretical[1,2] studies of first-order induced Raman scattering in alkali halides containing monovalent substitutional impurities have been made. Divalent impurities in the alkali halides present additional complications since the excess charge of the impurity must be compensated by an equal number of vacancies. Induced Raman scattering from NaCl:Ca^{2+} has been reported by Kaiser *et al.*,[3] from LiF:Mn^{2+} by Jain *et al.*,[4] and from LiF:Mn^{2+} and LiF:Mg^{2+} by Teng and Dugautier.[5] The scattering from isolated Ca^{2+} ions and from Ca^{2+}-vacancy aggregates was studied in the case of NaCl:Ca^{2+}, and the results were consistent with an assumed C_{2v} symmetry for the Ca^{2+}-vacancy association.[6]

Our initial purpose in investigating the induced Raman spectra of LiCl:Ni^{2+} was to obtain the frequencies of the $NiCl_6^{4-}$ complex so that interpretation of the vibronic fine structure observed[7] with the electronic transitions of Ni^{2+} in LiCl might be attempted. In this regard, we also tried to measure the impurity-induced infrared spectra, but these experiments were unsuccessful. In order to provide a basis for interpreting the observed Raman spectra of LiCl:Ni^{2+}, theoretical calculations were done for the first-order induced Raman scattering from the neighbors of both isolated substitutional Ni^{2+} ions and isolated cation vacancies.

II. EXPERIMENTAL PROCEDURES AND RESULTS

The single crystals of LiCl:Ni^{2+} were grown from mixtures of purified LiCl and $NiCl_2$ by a modified Bridgman technique.[7] Small crystals measuring about $5 \times 3 \times 1$ mm were cleaved from two larger specimens that contained, respectively, 0.2- and 0.4-wt% nickel, as determined by spectrographic analysis. These concentrations correspond to about 4×10^{19} and 9×10^{19} Ni^{2+}/cm^3, or to about 0.1 and 0.2 at.%, respectively. Cleaved samples with faces parallel to principal planes were denoted as ⟨100⟩ crystals. A ⟨110⟩ crystal was prepared by grinding and polishing two opposite faces parallel to the (110) planes. Because LiCl is hygroscopic, all preparations and mounting of samples onto the cold stage of a closed cycle refrigerator were carried out in polyethylene bags purged with dry air. Polarized Raman spectra of ⟨100⟩ and ⟨110⟩ crystals of LiCl:Ni^{2+} and of an undoped ⟨100⟩ crystal of LiCl were measured at 300 and at 12 K with the equipment described previously.[8] The 488.0-nm line of an argon-ion laser operating at ~800 mW was the excitation source, and spectra were recorded with spectral slit widths of either 1 or 2 cm^{-1}. Based on calibrations using the argon emission lines, the estimated accuracy of the measured frequencies for sharp bands was ±0.5 cm^{-1}.

Attempts were made to observe the impurity induced infrared spectrum of LiCl:Ni^{2+} by measuring the transmission of a thin single crystal (~0.2 mm thick) at 12 K using a Fourier-transform spectrometer. However, this sample was virtually totally absorbing in the far-infrared region of interest, i.e., between 100 and 300 cm^{-1}.[9]

Polarized Raman spectra of ⟨100⟩ and ⟨110⟩ crys-

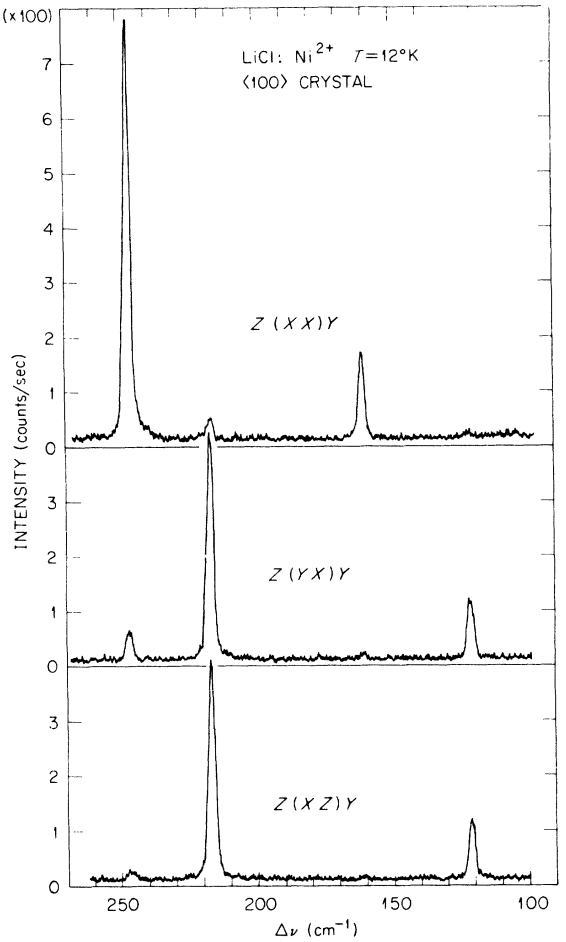

FIG. 1. Polarized first-order induced Raman spectra of a ⟨100⟩ LiCl:Ni^{2+} crystal using 488.0-nm excitation. Slit width ≃ 2 cm^{-1}.

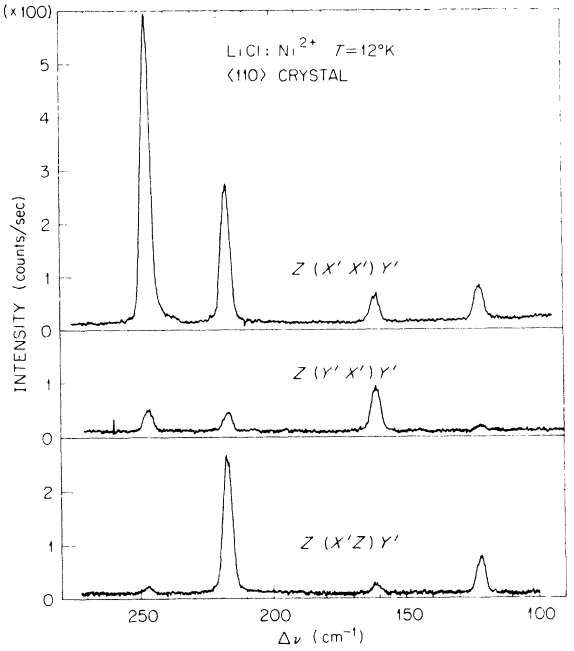

FIG. 2. Polarized first-order induced Raman spectra of a ⟨110⟩ LiCl:Ni^{2+} crystal using 488.0-nm excitation. Slit width ≃ 2 cm^{-1}.

tals of LiCl:Ni^{2+} (4×10^{19} Ni^{2+}/cm^3) measured at 12 K are shown in Figs. 1 and 2, respectively. No additional bands were observed below 100 cm^{-1}, and the features appearing above 300 cm^{-1}, which are not shown in these figures, are due to the second-order Raman spectrum. The frequencies and relative intensities (peak heights) of the bands observed in 100- to 250-cm^{-1} region are collected in Table I. The irreducible representations for the vibrational modes of an isolated species having O_h symmetry are given by[10] $\Gamma(O_h)=A_{1g}+E_g+T_{2g}+2T_{1u}+T_{2u}$. The scattering tensors for the g modes as given by Loudon[11] correspond to the ⟨100⟩ orientation. For this orientation, the A_{1g} and E_g modes are active in $z(xx)y$ scattering while the T_{2g} mode is active in $z(xz)y$, $z(yz)y$, and $z(yx)y$ scattering. The ⟨110⟩ orientation of the LiCl:Ni^{2+} crystal corresponds to a rotation of 45° about the z axis. It can be shown that[1] for this case, the A_{1g} mode is active in $z(x'x')y'$ scattering, the E_g mode is active in $z(x'x')y'$ and $z(y'x')y'$ scattering, and the T_{2g} mode is active in $z(x'x')y'$, $z(x'z)y'$, and $z(y'z)y'$ scattering. Thus, the E_g mode is distinguished by the fact that it is the only mode predicted to be active in $z(y'x')y'$ scattering.

The assignments of the bands given in Table I were based on their relative intensities in each of the polarized Raman spectra of the ⟨100⟩ and ⟨110⟩ crystals. The appearance of residual components, i.e., bands appearing in polarizations in which they are formally forbidden, may be caused by slight misalignment of the crystal and by the large solid angle at which the scattered light was collected.[8] As shown in Table I, the frequencies of the first-order induced Raman bands shift upward slightly as the temperature is lowered from 300 to 12 K. The widths[12] of these bands were ~10 cm^{-1} at 300 K and ~2 cm^{-1} at 12 K.

The electronic spectra of LiCl:Ni^{2+} show that the Ni^{2+} ions occupy Li^+ sites in the lattice.[7,13] In the absence of any perturbation, the symmetry of the $NiCl_6^{4-}$ complex in LiCl has O_h symmetry. However, the Li^+ vacancies required for charge compensation could lower the symmetry about the Ni^{2+} ions to C_{2v}, as in the case of divalent rare earth ions in alkali halides.[6] The possibility of forming different types of defects was considered in the case[3] of NaCl:Ca^{2+}. These types were taken to be (i) isolated defects in which the cation vacancy is sufficiently far removed as to have a negligible effect on the defect; (ii) associations of one

TABLE I. Frequencies and relative intensities of the first-order induced Raman bands of $LiCl:Ni^{2+}$.

Frequency (cm^{-1}) $T=12$ K	⟨100⟩ Orientation Relative intensity [a] $z(xx)y$	$z(xz)y$	$z(yz)y$	$z(yx)y$	Symmetry (O_h)
247	100	4	7	15	A_{1g}
216	5	61	55	56	T_{2g}
161	19	1	1	4	E_g
122	5	16	16	16	T_{2g}

Frequency (cm^{-1}) $T=300$ K	$T=12$ K	⟨110⟩ Orientation Relative intensity [a] (12 K) $z(x'x')y'$	$z(x'z)y'$	$z(y'z)y'$	$z(y'x')y'$	Symmetry (O_h)
240	247	100	2	13	7	A_{1g}
212	216	44	44	50	6	T_{2g}
155	161	9	3	2	14	E_g
116	122	11	12	12	2	T_{2g}

[a] Peak heights in arbitrary units normalized to 100 for the strongest band.

divalent impurity and one vacancy; and (iii) aggregates of these associations. It was assumed that at low-impurity concentrations, the latter defect need not be considered. It was observed that Raman spectra of quenched $NaCl:Ca^{2+}$ crystals were different from those of annealed crystals. The observed bands of the isolated defects in quenched crystals were assigned according to O_h symmetry, while the bands of the associated defect-vacancy center in annealed crystals were assigned according to C_{2v} symmetry. The formation of different types of defect centers in $LiCl:Ni^{2+}$ was studied previously.[7] Unlike the case of $NaCl:Ca^{2+}$, it was found that the electronic spectra of $LiCl:Ni^{2+}$ crystals quenched to room temperature from 623 K were essentially identical to the spectra of crystals which were slowly cooled to room temperature. These results indicate that predominantly one type of defect is formed in $LiCl:Ni^{2+}$ at the concentrations of Ni^{2+} used in this study. As noted above, except for the difference in the total intensity, the Raman spectra of crystals with different Ni^{2+} concentrations were identical as far as the four bands reported in Table I are concerned. It seems reasonable, therefore, to associate the observed first-order induced Raman spectra of the crystals examined here with isolated Ni^{2+} ions and/or isolated Li^+ vacancies.

If it is assumed that only the vibrational modes of the $NiCl_6^{4-}$ octahedral complex are important, the observed spectrum should show only one T_{2g} band instead of the two that are observed. The additional T_{2g} band, at the very least, must then be assigned to the Li^+ vacancy or to an octahedral complex larger than Ni^{2+} and its six nearest-neighbor Cl^- ions. Since Li^+ is expected to have a small induced polarizability, the larger complex would have to extend at least out to third neighbors of the defect. This points out a fundamental difficulty in interpreting first-order Raman spectra in crystals containing charge-compensated impurities, namely, the problem of identifying which features are due to the impurity and which are due to the compensating defect. The theoretical study outlined in Sec. III was undertaken in an attempt to resolve this uncertainty.

Before describing the theoretical calculations, it is useful to consider the possibility that, in spite of the evidence from the electronic spectra, a Ni^{2+} ion and its charge-compensating Li^+ vacancy are so closely associated that the O_h symmetry of the $NiCl_6^{4-}$ complex is destroyed. If it is assumed that the symmetry of the complex is lowered to C_{2v} by the Li^+ vacancy at a nearest-neighbor cation site,[6] then the irreducible representations of the vibrational modes of the $NiCl_6^{4-}$ group are given by $\Gamma(C_{2v}) = 4A_1 + 3A_2 + 4B_1 + 4B_2$. All of these modes are Raman active, and thus the spectrum predicted for a C_{2v} structure is expected to be far more complex than that observed. Attempts to account for the extra Raman band by lowering the symmetry from O_h showed that only a reduction to O symmetry[14,15] would account for four Raman bands while all other symmetries required more than four Raman bands. It is not possible, however, to construct a defect center consisting of the $NiCl_6^{4-}$ complex and a cation vacancy which has this symmetry.

III. THEORY AND METHODS OF CALCULATION

Our calculations of the first-order induced Raman scattering from $LiCl:Ni^{2+}$ are based on

localized perturbation theory. Since this theory and the computational procedures involved in our application of it have been described in detail elsewhere,[1,16] only a brief discussion will be presented here in order to clarify the presentation of the calculated results in Sec. IV.

Localized-perturbation theory assumes that the addition of an impurity atom to or the removal of an ion from the host lattice affects only a relatively small region of the lattice around the defect site. The equations of motion of a crystal containing a single substitutional impurity or vacancy in an otherwise perfect lattice are given in matrix form by

$$[(\underline{M}_0+\delta\underline{M})\omega^2-(\underline{K}_0+\delta\underline{K})]\underline{u}=\underline{0}\,, \tag{1}$$

where $\underline{M}_0$ and $\underline{K}_0$ are, respectively, the mass and force constant matrices of the unperturbed lattice, $\delta\underline{M}$ and $\delta\underline{K}$ are matrices of the mass and force constant changes due to the defect, and $\underline{u}$ is the vector of Cartesian displacements. The elements of the force constant matrix, $\underline{K}_0$ are given (in the harmonic approximation) by

$$K_{\alpha\beta}(l\kappa,l'\kappa')=\left(\frac{\partial^2\Phi}{\partial u_\alpha(l,\kappa)\partial u_\beta(l'\kappa')}\right)_0, \tag{2}$$

where α labels the component of the displacement u of the κth ion in the lth cell, and the derivatives of the total crystal potential Φ are evaluated at the equilibrium ionic positions. Equation (1) can be cast into a different form, i.e.,

$$(1+\underline{G}^\circ\underline{\Delta})\underline{u}=0\,, \tag{3}$$

where $\underline{G}^\circ=(\underline{M}_0\omega^2-\underline{K}_0)^{-1}$ is the Green's-function matrix for the perfect crystal, and $\Delta=\delta\underline{M}\omega^2-\delta\underline{K}$ is often referred to as the defect matrix. The Green's-function matrix of the perturbed crystal can then be expressed in terms of $\underline{G}^\circ$ and $\underline{\Delta}$ by

$$\underline{G}=[(\underline{M}_0\omega^2-\underline{K}_0)+\underline{\Delta}]^{-1}=(1+\underline{G}^\circ\underline{\Delta})^{-1}\underline{G}^\circ. \tag{4}$$

It can be shown[16] that the intensity of Raman scattering at 0 K is proportional to terms of the form

$$I_{\alpha\gamma,\beta\lambda}=\sum_{\nu,l}\sum_{\mu,l'}\frac{\partial P_{\alpha\gamma}}{\partial u_\nu(l)}\frac{\partial P_{\beta\lambda}}{\partial u_\mu(l')}\times\mathrm{Im}\langle\nu l\,|\,\underline{G}(\omega^2+i0^+)\,|\,\mu l'\rangle\,, \tag{5}$$

where $\mathrm{Im}\langle\nu l\,|\,\underline{G}(\omega^2+i0^+)\,|\,\mu l'\rangle$, the imaginary part of a matrix element of $\underline{G}$, is to be evaluated in the limit as ω approaches the real axis from above. The derivatives of the elements of the polarizability tensor $P_{\alpha\gamma}$, with respect to the Cartesian-displacement coordinates of the ions are treated as parameters in the present calculations. For the purpose of calculating the Raman scattering, it is more convenient[17] to express Eq. (5) in terms of symmetrized displacement coordinates, which are linearly related to the u's. The symmetrized coordinates are basis functions of the point group which describes the symmetry about the defect (O_h in the case of LiCl:Ni^{2+}), and the defect matrix $\underline{\Delta}$ in Eq. (3) has nonvanishing elements only within the "defect space" defined by these coordinates.

As shown by Eq. (4), in order to calculate the matrix elements of $\underline{G}$ in Eq. (5), it is necessary to determine $\underline{G}^\circ$ and $\underline{\Delta}$. The calculation of the matrix elements of $\underline{G}^\circ$ requires knowledge of the eigenfrequencies and eigenvectors of the perfect crystal. These can be obtained from some model for the lattice dynamics of the perfect crystal, e.g., the shell model. Unfortunately, reliable shell model parameters are lacking for LiCl because the phonons have not yet been measured by neutron scattering. The only shell-model parameters available for LiCl are those obtained by Haridasan[18] from optical and elastic constant data. Although these were used in our calculations, they may not give a good fit to the phonon dispersion curves throughout the Brillouin zone and this could easily lead to substantial differences between the computed and measured Raman spectra.

The model used to obtain estimates of the force-constant changes $\underline{\Delta}$ has been described elsewhere[17] and only its main features will be given here. The ions of the host crystal in the region neighboring the impurity are treated electrically as point charges and point dipoles, and the repulsive interactions are taken to be of the Born-Mayer exponential form. The crystal outside of this inner region is treated as a polarizable continuum for the purpose of calculating the electronic and displacement dipoles induced by the presence of the impurity. The impurity itself is also represented electrically by a point charge which has Born-Mayer repulsive interactions with its neighbors. The inner region can be made large enough (in the computer program) to include the four nearest-neighbor shells of ions around the impurity. Once the extent of the inner region has been chosen, the ions within it are allowed to relax (in an A_{1g} configuration) until the energy of the impurity-host complex is minimized. The second derivatives for A_{1g}, E_g, and T_{2g} displacements from the new-equilibrium position are then computed. The difference between these symmetrized force constants and those found when a normal host ion occupies the impurity site gives the elements of the defect matrix $\underline{\Delta}$.

We do not expect the results obtained from this model to give us more than semiquantitative results for the LiCl:Ni^{2+} system. One difficulty lies in our lack of satisfactory Born-Mayer parameters for the Ni^{2+}-Cl^- interaction. In fact, we have taken these to be the same as for the Li^+-Cl^- interaction.

This problem is minimized somewhat for the A_{1g} modes by the strong Coulomb forces between the impurities (Ni^{2+} and vacancy) and the ions of the host lattice. However, this strong, long-range interaction is the source of another difficulty, since it is not likely to lead rigorously to a defect matrix Δ of small dimensions for all irreducible representations. In the calculation of the matrix elements of Δ with the classical ionic crystal model, long-range forces between the ions are included. Furthermore, those long-range effects which are neglected by the truncation of the defect space can be partially taken into account by our parametrization of the short-range perturbations. In our calculations, the Born-Mayer parameters for LiCl were taken from the work of Tosi and Fumi[19] (first set of data in Table I) and the ionic polarizabilities from Tessman, Kahn, and Schockley.[20]

IV. RESULTS OF CALCULATION AND DISCUSSION

The results of the force constant calculations for the Ni^{2+} ion and the vacancy are given in Table II for the case in which the displacements of the first and fourth neighbors constitute the defect space. Qualitatively similar results are obtained when the defect space is enlarged to include second- and third-neighbor displacements. It is seen that, whereas the A_{1g} force constant for the displacement of the first-nearest-neighbor Cl^- ions around an Ni^{2+} ion shows a large increase as expected, the corresponding E_g force constant exhibits a large decrease. When these force-constant changes are used to calculate the Raman-scattering cross section, a sharp peak (resonance) is obtained for the A_{1g} mode but none for the E_g. The reverse situation occurs around the vacancy, i.e., the 1, 1 A_{1g} element of the force constant matrix decreases, the corresponding element of the E_g matrix increases, and the Raman cross section shows a sharp resonance for the E_g mode but none for the A_{1g} mode.

TABLE II. Calculated estimates of the force constant changes around Ni^{2+} ions and Li^+ vacancies. Symmetrized coordinates constructed from the displacements of the first- and fourth-nearest neighbors of the defect were used here.

Shells	A_{1g}	E_g	T_{2g}
Force-constant changes [a] around Ni^{2+}			
1,1	+48 659	−45 200	+25 445
1,4	+6 583	+23 369	2 145
4,4	−5 226	−1 572	−495
Force-constant changes [a] around Li^+ vacancy			
1,1	−8 525	24 924	+12 293
1,4	−14 726	−31 245	−1 632
4,4	+9681	6 327	−5 576

[a] Force-constant changes in dyn/cm.

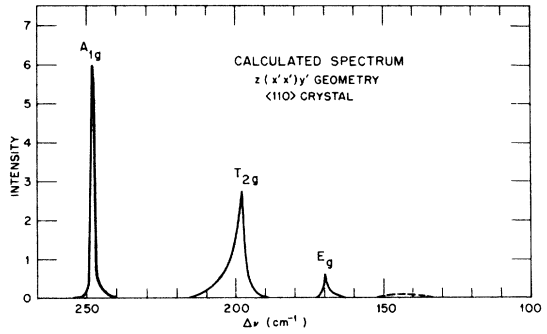

FIG. 3. Calculated spectrum obtained as described in the text. The dashed curve is weak structure associated with the E_g peak.

With the results of Table II as a guide, the 1, 4 and 4, 4 force constant changes were set equal to zero, and the 1, 1 change was varied until approximate agreement with the experimental data was obtained. The values obtained in this way were $\Delta K_{11}(A_{1g}) = 74\,500$ dyn/cm (around Ni^{2+}) and $\Delta K_{11}(E_g) = 22\,000$ dyn/cm (around an Li^+ vacancy). The calculated Raman spectrum using these force constant changes is shown in Fig. 3. The intensities of the peaks were adjusted separately to agree approximately with the ratios found experimentally for the $z(x'x')y'$ geometry in the $\langle 110 \rangle$ orientation. The calculated Raman intensities do not give these ratios since the polarizability derivatives for the modes are not specified by the theory used here. The lack of experimentally measured phonon-dispersion curves for LiCl makes it difficult to justify more involved calculations in which the 1, 4 and 4, 4 force constant changes are also varied. For the same reason we are not particularly concerned about the exact position of the peaks, their shapes, or the additional weak structure associated with the E_g peak (dashed curve on Fig. 3). The results of these calculations strongly suggest that although the A_{1g} peak comes from the neighbors of the Ni^{2+} ion, the E_g peak is produced by the presence of Li^+ vacancies.

The results given in Table II for the T_{2g} modes show a large force-constant change for the first-nearest-neighbor ions around the Ni^{2+} ions. We found that $K_{11}(T_{2g}) = 38\,000$ dyn/cm would place a peak close to the experimentally observed position. Although this peak is substantially broader than the experimental one, the result suggests that the T_{2g} mode observed at 216 cm^{-1} is due to a local or quasilocal mode around the Ni^{2+} ions. The situation with the T_{2g} mode around the Li^+ vacancy

is less satisfactory. The calculated 1,1 force constant change around the vacancy is about one-half that for the Ni^{2+} ion. The calculations indicated that a strong interaction should occur between the T_{2g} vacancy mode and the perfect crystal modes in the acoustical region, and that the Raman spectrum should show structure over a broad frequency range. The observed spectrum, however, showed only a single sharp band at 122 cm^{-1} in this region (Figs. 1 and 2). For clarity, we have not shown the calculated results for the low-frequency T_{2g} mode in Fig. 3 because they extend over such a wide frequency range. In order to bring the calculated and observed spectra into agreement, it would be necessary to find a set of force-constant changes which induce a single sharp resonancelike mode at the observed position in the acoustical region. It is by no means certain that this can be done with Haridasan's shell model for LiCl and with the further approximations we have made in our calculations. Hence, we are unable to show conclusively that our assignment of the bands is correct although the evidence for it from the A_{1g} and E_g modes seems rather strong.

---

†Research sponsored by the U.S. Energy Research and Development Administration under Contract with Union Carbide Corp.

*Department of Chemistry, Angelo State University, San Angelo, Tex. 76901.

[1]For example, see G. P. Montgomery, Jr., M. V. Klein, B. N. Ganguly, and R. F. Wood, Phys. Rev. B 6, 4047 (1972).

[2]For example, see A. M. Karo and J. R. Hardy, Phys. Rev. B 12, 690 (1975).

[3]R. Kaiser, W. Spengler, and W. Möller, Phys. Status Solidi B 55, 659 (1973).

[4]K. P. Jain, S. Radhakrishna, and A. K. Prabhakaran, Phys. Rev. B 5, 2325 (1972).

[5]M. Teng and C. Dugautier, C. R. Acad. Sci. (Paris) B 269, 1109 (1969).

[6]W. E. Bron and W. R. Heller, Phys. Rev. 136, A1433 (1964).

[7]G. E. Shankle, Ph.D. thesis (University of Tennessee, 1969) (unpublished); and ORNL Report No. ORNL-TM-2514 (1969) (unpublished).

[8]J. B. Bates and J. C. Pigg, J. Chem. Phys. 62, 4227 (1975).

[9]The fundamental transverse-optical mode of LiCl has been measured at 191 cm^{-1} by reflection; cf. M. Hass, J. Phys. Chem. Solids 24, 1159 (1963).

[10]G. Herzberg, *Infrared and Raman Spectra* (Van Nostrand, New York, 1945), p. 122.

[11]R. Loudon, Adv. Phys. 13, 423 (1964).

[12]Full width at one-half band maximum.

[13]K. Polák and M. Lèbl, Czech. J. Phys. B 22, 1179 (1972).

[14]The O group is isomorphous to the T_d group, but the correlation to the triply degenerate species are different; cf. Ref. 10, p. 121.

[15]E. B. Wilson, Jr., J. C. Decius, and P. C. Cross, *Molecular Vibrations* (McGraw-Hill, New York, 1955), Appendix X.

[16]R. F. Wood, *Methods in Computational Physics*, edited by B. Adler, S. Fernbach, and M. Rotenberg (Academic, New York, 1976), Vol. 15, p. 119.

[17]M. Mostoller and R. F. Wood, Phys. Rev. B 7, 3935 (1973).

[18]T. M. Haridasan, Opt. Commun. 9, 296 (1973).

[19]M. P. Tosi and F. G. Fumi, J. Phys. Chem. Solids 25, 45 (1964).

[20]J. R. Tessman, A. H. Kahn, and W. Shockley, Phys. Rev. 92, 890 (1953).